Biochimica et Biophysica Acta 1808 (2011) 2036–2044

Contents lists available at ScienceDirect

Biochimica et Biophysica Acta

journal homepage: www.elsevier.com/locate/bbamem

Volume regulation of murine T lymphocytes relies on voltage-dependent and two-pore domain potassium channels

Nicole Bobak [a,b], Stefan Bittner [a,b], Joseph Andronic [c], Susanne Hartmann [c], Friederike Mühlpfordt [c], Tilman Schneider-Hohendorf [a,b], Karen Wolf [c], Carsten Schmelter [c], Kerstin Göbel [a,b], Patrick Meuth [d], Heiko Zimmermann [e,f], Frank Döring [g], Erhard Wischmeyer [g], Thomas Budde [d], Heinz Wiendl [a,b], Sven G. Meuth [a,b,*,1], Vladimir L. Sukhorukov [c,1]

[a] University of Muenster, Department of Neurology — Inflammatory Disorders of the Nervous System and Neurooncology, Domagkstr, 13, 48149 Muenster, Germany
[b] Institute of Physiology — Neuropathophysiology, Domagkstr, 13, 48149 Muenster, Germany
[c] University of Wuerzburg, Department of Biotechnology and Biophysics, Biozentrum, Am Hubland, 97074 Wuerzburg, Germany
[d] University of Muenster, Institute of Physiology I, Robert-Koch-Str. 27a, 48149 Muenster, Germany
[e] Fraunhofer Institute for Biomedical Engineering (IBMT), Ensheimer Str. 48, 66386 St. Ingbert, Germany
[f] Saarland University, Department of Molecular & Cellular Biotechnology/Nanotechnology, Campus, 66123 Saarbrücken, Germany
[g] University of Wuerzburg, Institute of Physiology, Röntgenring 9, 97070 Wuerzburg, Germany

ARTICLE INFO

Article history:
Received 15 January 2011
Received in revised form 22 April 2011
Accepted 25 April 2011
Available online 5 May 2011

Keywords:
Cell volumetry
Regulatory volume decrease
Osmotic stress
T lymphocyte
Potassium channel
K_{2P} channels

ABSTRACT

A variety of ion channels are supposed to orchestrate the homoeostatic volume regulation in T lymphocytes. However, the relative contribution of different potassium channels to the osmotic volume regulation and in particular to the regulatory volume decrease (RVD) in T cells is far from clear. This study explores a putative role of the newly identified K_{2P} channels (TASK1, TASK2, TASK3 and TRESK) along with the voltage-gated potassium channel $K_V1.3$ and the calcium-activated potassium channel $K_{Ca}3.1$ in the RVD of murine T lymphocytes, using genetic and pharmacological approaches. K_{2P} channel knockouts exerted profound effects on the osmotic properties of murine T lymphocytes, as revealed by reduced water and RVD-related solute permeabilities. Moreover, both genetic and pharmacological data proved a key role of $K_V1.3$ and TASK2 channels in the RVD of murine T cells exposed to hypotonic saline. Our experiments demonstrate a leading role of potassium channels in the osmoregulation of T lymphocytes under different conditions. In summary, the present study sheds new light on the complex and partially redundant network of potassium channels involved in the basic physiological process of the cellular volume homeostasis and extends the repertoire of potassium channels by the family of K_{2P} channels.

1. Introduction

Volume regulation is a vital ability of cells which is challenged by a variety of factors such as alterations of the extracellular osmolality, activation of membrane channels and transporters, synthesis or cleavage of cytosolic proteins and cell metabolism. Changes in the osmotic conditions and the resulting osmotic pressure gradients cause water to move rapidly through the plasma membrane, thus leading to cell swelling or shrinkage [1–3]. Thereafter, the return to the original cell volume may result from the movement of ions and small organic osmolytes across the cell membrane.

A multitude of cell volume regulating mechanisms is known to be used by various cell types. There is a general agreement that regulatory volume decrease (RVD) in hypotonically swollen lymphocytes mainly relies on the cytosolic efflux of chloride (Cl^-) and potassium (K^+) ions [4]. T lymphocytes possess swelling-activated chloride channels (Cl_{swell}) of yet enigmatic molecular identity [4,5]. Hypotonic cell swelling induces the activation of these ATP-dependent Cl_{swell} currents. In consequence RVD gets initiated and leads back to the normal cell size even though the hypotonicity persists [6]. The efflux of Cl^- ions causes membrane depolarization which opens voltage-gated potassium channels ($K_V1.3$) [7–9]. Within several minutes, the efflux of anions and cations along with the osmotically driven water loss results in a shrinkage of the cell back to its original isotonic volume. Besides voltage-gated potassium channels, calcium-activated potassium channels ($IK_{Ca}1 = K_{Ca}3.1$) can be involved in RVD

Abbreviations: CGM, complete growth medium; K_{2P}, two-pore-domain potassium channels; MACS, magnetic cell separation; PDMS, polydimethylsiloxane; PBS, phosphate buffered saline; RVD, regulatory volume decrease; RVI, regulatory volume increase; ShK, *Stichodactyla* toxin; TRAM34, 1-[(2-Chlorophenyl)diphenylmethyl]-1H-pyrazole; Wt, wild type

* Corresponding author at: University of Muenster, Department of Neurology — Inflammatory Disorders of the Nervous System and Neurooncology, Domagkstr, 13, 48149 Muenster, Germany. Tel.: +49 251 83 46811; fax: +49 251 83 46812.
E-mail address: sven.meuth@ukmuenster.de (S.G. Meuth).

[1] Equal contributions by senior authors (S.G. Meuth and V.L. Sukhorukov).

0005-2736/$ – see front matter © 2011 Elsevier B.V. All rights reserved.
doi:10.1016/j.bbamem.2011.04.013

as well, which is, however, controversially discussed in the literature. In mature T cells, RVD has been reported either to be Ca^{2+} independent [10,11] or to involve $IK_{Ca}1$ channels [12,13]. Moreover, an activation of $IK_{Ca}1$ by swelling-activated Ca^{2+} channels seems to occur in mouse thymocytes [4,14]. This is in accordance with the predominant expression of another type of voltage-gated potassium channels ($K_V3.1$ instead of $K_V1.3$) in mouse thymocytes [15–17]. Interestingly, transfection of a volume-regulation deficient cell line with $K_V3.1$ does not confer the ability to RVD in these cells [8]. Additionally, several alternative pathways have been suggested to contribute to the volume regulation in lymphocytes, including a putative involvement of TRPM7 channels [4,18,19], taurine efflux pathways [20] or swelling-activated channels for organic osmolytes [21,22].

Recent studies have emphasized the emerging role of newly identified members of the two-pore domain (K_{2P}) potassium channel family in lymphocytes. These are TASK1, TASK2 and TASK3 which are expressed in human and mouse T lymphocytes [23,24], TRESK in Jurkat cells [25,26] and TREK2 in mouse B lymphocytes [27]. Given that TASK channels are mostly time- and voltage-independent they are well-suited to carry a background K^+ conductance while TRESK channels are calcium-activated. In light of the new developments in the K_{2P} channel research, this study explores the role of various types of potassium channels in the volume regulation of mouse T lymphocytes subjected to hypo- and hypertonic saline solutions, using a combination of pharmacological and genetic approaches.

2. Materials and methods

2.1. Cell isolation and incubation

Murine splenocytes were isolated from adult transgenic and wild type (wt) mice following standard procedures and $CD4^+$ T lymphocytes were separated by magnetic cell separation (MACS) using $CD4^+$ T cell isolation kit II (Miltenyi, Germany). These T cells were suspended in splenocyte complete medium (DMEM, 10 mM HEPES, 50 μM β-mercaptoethanol, 5% FCS, 2 mM L-Glutamine and 1% nonessential amino acids (NEAA)) and cultured at 37 °C, 5% CO_2 atmosphere for 48 h with CD3/CD28 mouse T activator Dynabeads (cell to bead ratio 4:1; Invitrogen).

2.2. Transgenic mice and reagents

C57BL/6 mice were purchased from Harlan Winkelmann (Borchen, Germany). Wild type C3H and $TRESK^{-/-}$ [28], $TASK1^{-/-}$, $TASK3^{-/-}$ [29] and $TASK2^{-/-}$ mice [30] have been described before. Mice were bred and housed under specific pathogen-free conditions in the animal facilities of the Department of Neurology in Wuerzburg according to German guidelines for animal care. Channel blockers (all from Sigma, Germany, except ShK, which was from Bachem AG, Switzerland) were used in the following concentrations: anandamide 30 μM (TASK1), quinidine 20 μM (TASK2) or 50 μM (TRESK), spermine 500 μM (TASK3), ShK 10 nM ($K_V1.3$), TRAM34 100 nM ($IK_{Ca}1$).

2.3. Cell volumetry

Cell volume changes were measured by video microscopy using a flow chamber designed for rapid exchange of media. The transparent body and floor of the chamber were made of polydimethylsiloxane (PDMS) and a 0.15 mm thick glass coverslip, respectively. To enhance cell adhesion, the coverslip was pretreated for 5–10 min with 0.5 mg/ml poly-D-lysine (Sigma, Germany). At a flow rate of about 1 ml/min the exchange of solutions in the chamber took about 2 s from the moment of turning the tap. Before measuring, an aliquot of cells suspended in isotonic complete growth medium (CGM; ~330 mOsm) at a density of about 10^5 cells/ml was injected into the chamber and the cells were allowed to settle and adhere to the chamber floor for 10–15 min. The chamber was placed on the stage of a microscope (BX50, Olympus, Hamburg, Germany) and the cells were viewed with a 20× objective in transmitted light. The microscope was equipped with a CMOS video camera (UI-1410-C, UEye, Obersulm, Germany) connected to the video digitizing board of a personal computer. Cell images were taken ~1 min before and at various time intervals from 10 s up to ~20 min after medium exchange. The cross-section areas of typically 8–10 cells per microscopic field were determined with the image analysis program ImageJ (Wayne Rasband, NIH, Maryland, USA). At each time interval, the volume (V) of an individual cell (Fig. 1) was evaluated from its cross-section by assuming spherical geometry. The cell volume was normalized to the original isotonic volume (V_0) as: $\nu = V/V_0$. In each experiment, the mean ν values (±SE) were calculated from a sequence of about 160 images and plotted against time after the change from isotonic CGM to a PBS (phosphate buffered saline) solution of varying osmolality.

The PBS solutions of osmolalities 200, 330, 400 and 450 mOsmol/kg were prepared by dilution of 10× Dulbecco's PBS (without Ca^{2+} and Mg^{2+}; PAA, Linz, Austria) with appropriate amounts of deionized water from a Milli-Q purification system (Millipore GmbH, Schwalbach, Germany). The solution osmolality (mOsmol/kg, denoted hereafter as mOsm) was measured by means of the cryoscopic osmometer Osmomat 010 (Gonotec, Berlin, Germany).

2.4. Analysis of the volumetric data

To analyze the effects of potassium channel blockers and K_{2P} gene knockouts on volume regulation (generally for hypotonic conditions) we used the following equation to calculate the RVD inhibition index IC_{RVD}:

$$IC_{RVD} = \left(\frac{\nu_{12} - \nu_0}{\nu_2 - \nu_0}\right) * 100\% \quad (1)$$

where $\nu_0 = 1$ is the normalized isotonic volume. The symbols ν_2 and ν_{12} stand for the normalized cell volumes 2 and 12 min after cell transfer into hypotonic medium (as depicted in Fig. 2). For cell samples accomplishing RVD within 12 min ($\nu_{12} = \nu_0 = 1$), Eq. (1) yields $IC_{RVD} = 0$ (i.e. no RVD inhibition). Cells exhibited $IC_{RVD} = 100\%$ if they remained swollen in hypotonic medium ($\nu_{12} = \nu_2$) and thus were incapable of RVD. In several experiments, continuous secondary swelling occurred after the fast initial volume increase, i.e. $\nu_{12} > \nu_2$. In those cases, IC_{RVD} was larger than 100%.

We additionally applied the modified osmoregulation model proposed by Lúcio et al. [31], to analyze quantitatively the membrane transport properties in lymphocytes subjected to hypotonic shock. Besides considering the standard osmotic water flux, the Lúcio-model assumes a cell volume-dependent solute permeability of the plasma membrane which in turn allows for the regulatory volume changes. The theory by Lúcio et al. [31] leads to the following simplified expression for the absolute cell volume $V(t)$ as function over time after hypotonic shock:

$$V(t) = Ae^{-t/\tau_1} - Be^{-t/\tau_2} + V_R, \quad (2)$$

where $A = \frac{(V_0 - V_b)\Delta\phi_0}{\phi_e}$, $B = \frac{(V_0 - V_b)\Delta\phi_0}{\phi_e} + (V_R - V_0)$, $\tau_1 = \frac{\varrho_w (V_0 - V_b)}{P_w A_0 \phi_e}$ and $\tau_2 = \frac{\phi_e V_0}{\alpha A_0}$. Symbols V_0 and V_b stand, respectively, for the initial cell volume and the osmotically inactive volume, both for isotonic conditions (~330 mOsm). For the initial conditions, $\Delta\phi_0$ is the osmotic shock, i.e. the initial difference between the extra- and intracellular osmolalities $\Delta\phi_0 = (\phi_e - \phi_i)$. The total membrane area $A_0 = 4\pi r_0^2$ is assumed invariable during the osmotic shock. The isotonic cell radii r_0 were evaluated from the microphotographs, such as shown in Fig. 1. The molar water density is given by $\rho_w = 1/18$ mol cm^{-3}. The residual

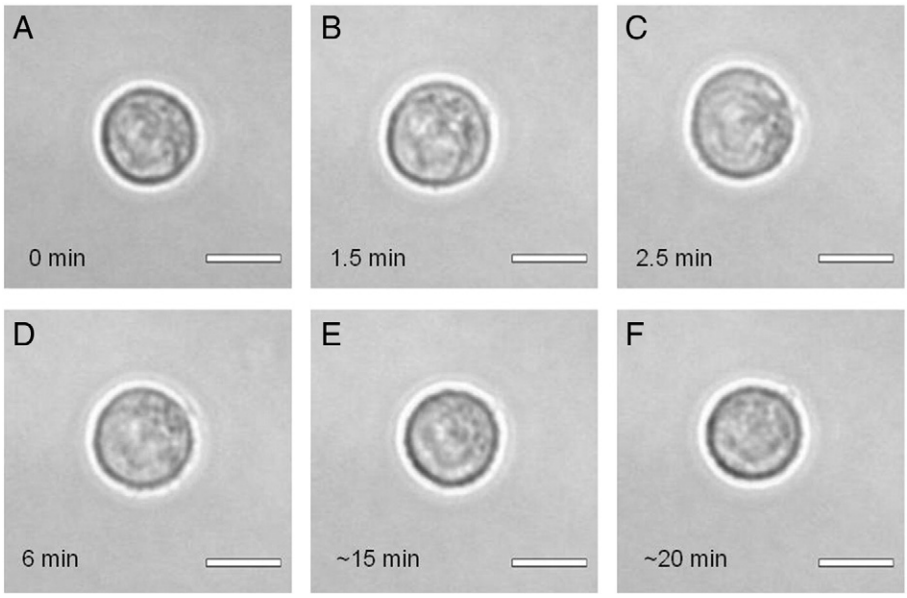

Fig. 1. Fast swelling and regulatory volume decrease (RVD) of a murine CD8$^+$ lymphocyte in 200 mOsm PBS (shown as a typical example). The microphotographs show the same cell before (A, isotonic CGM) and after acute hypotonic challenge (B–F) at the indicated time intervals. In isotonic CGM (A), the cell had a radius $r_0 \approx 3.1$ μm, corresponding to the original isotonic volume $V_0 \approx 0.12$ pL. Upon medium replacement the cell swelled to $V_{max} \approx 0.23$ pL (~3.8 μm) within 2.5 min (C) and then gradually shrank to nearly isotonic size within 6–20 min (C–F). Scale bar = 5 μm.

volume V_R is a final equilibrium volume achieved after the osmotic shock and RVD. The characteristic time τ_1 describes the initial cell swelling due to the water influx ("water phase"), whereas τ_2 is associated with the osmolyte release during RVD. Accordingly, τ_1 is inversely proportional to the osmotic water permeability P_w [μm s^{-1}] and τ_2 to the swelling-activated solute permeability α [mol s^{-1} cm^{-2}].

Best least-square approximations of the Lúcio-model to the volumetric data were calculated using a nonlinear regression procedure provided by Origin 8 (Microcal, Northampton, MA, USA). In general, the model contains four unknown parameters: b, P_w, α and V_R. All other quantities appearing in the model are fixed or known. In the hypotonic experiments with 200 mOsm PBS, ϕ_e and ϕ_i were 200 and 330 mOsm, respectively. The original isotonic cell volume V_0 and cell surface area A_0 (assumed invariable) were evaluated microscopically (Fig. 1). In order to reduce the number of unknown parameters, the osmotically inactive volume b was determined independently from the Boyle van't Hoff plot (see Fig. 3). The time-dependent cell volume $V(t)$ was the fitted variable. Despite its simplicity, the model matched well the observed volumetric behavior of hypotonically treated lymphocytes (see continuous curves in Figs. 2 and 4), thus allowing the quantitative estimation of membrane parameters in terms of solute and water permeabilities (α and P_w).

3. Results and discussion

3.1. Volumetry of CD4$^+$ and CD8$^+$ lymphocytes from wild type mice

The CD4$^+$ and CD8$^+$ T cell subpopulations derived from wild type mice exhibited quite similar volumetric responses to PBS over a wide tonicity range from 200 to 450 mOsm (wt in Fig. 2A and B). Under isotonic conditions (*triangles* in Fig. 2), i.e. upon cell transfer from 330 mOsm CGM to PBS of the same osmolality, gradual cell shrinkage occurred in both cell phenotypes for at least 15–20 min after medium exchange. This long-term volume decrease implies continuing leakage of intracellular solutes through the plasma membrane of cells bathed in isotonic Ca^{2+}-free PBS.

A sudden exposure to hypotonic 200 mOsm PBS caused both cell phenotypes to swell rapidly within the first 2 min (from $v_0 = 1$ to the maximum volume v_2) due to the water uptake driven by the imposed osmotic gradient (*open circles* in Fig. 2). The magnitude of initial swelling $v_2 = 1.24 \pm 0.02$ in CD8$^+$ cells was somewhat larger than in CD4$^+$ cells ($v_2 \approx 1.19 \pm 0.03$, see Fig. 2A and B, and Table 1). Afterwards, the cells shrank slowly to their original isotonic volume, despite persisting hypotonicity. Since both T cell subtypes from wt mice completed RVD 12 min after hypotonic challenge ($v_{12} \approx 1.0$), this time interval was used as reference for assessing the inhibitory effects of gene knockouts and channel blockers on RVD using Eq. (1) (see Section 2.4).

In sharp contrast to their efficient hypotonic volume regulation, neither CD4$^+$ nor CD8$^+$ cells were capable of undergoing regulatory volume increase (RVI) in hypertonic PBS (*filled symbols* in Fig. 2A and B). During the first 2–3 min upon hypertonic treatment, the cells underwent fast initial shrinkage, whose magnitude (v_0–v_2) grew with increasing PBS osmolality. After that, little – if any – changes in cell volume took place during the following 15–20 min. The observed lack of RVI in murine T lymphocytes reported here corroborates previous findings that lymphoid cells (e.g. human peripheral blood lymphocytes, mouse T lymphocytes, etc.) remain shrunken in hypertonic media for extended periods, with no observable RVI [9,32].

To estimate the osmotically inactive volume fraction in murine T lymphocytes, the experimental v_2 values were plotted against the reciprocal normalized osmolality (symbols in Fig. 3) and fitted by the Boyle van't Hoff equation:

$$v_2 = \frac{\varphi_{iso}}{\varphi}(1-b) + b \qquad (3)$$

where φ is the PBS osmolality and $\varphi_{iso} = 330$ mOsm is the isotonic osmolality. The term $b = V_b/V_0$ represents the osmotically inactive volume fraction at 330 mOsm. Judging by the correlation coefficient ($r = 0.98$), the *initial* osmotic response of murine T cells is well described by the linear Boyle van't Hoff relationship. The linear regression of Eq. (3) to the volumetric data yielded very similar estimates of the osmotically inactive fraction for CD4$^+$ ($b = 0.67 \pm 0.04$) and CD8$^+$ cells ($b = 0.68 \pm 0.02$). These b values were used to fit the Lúcio-model (Eq. (2)) to the volumetric data shown in Fig. 2.

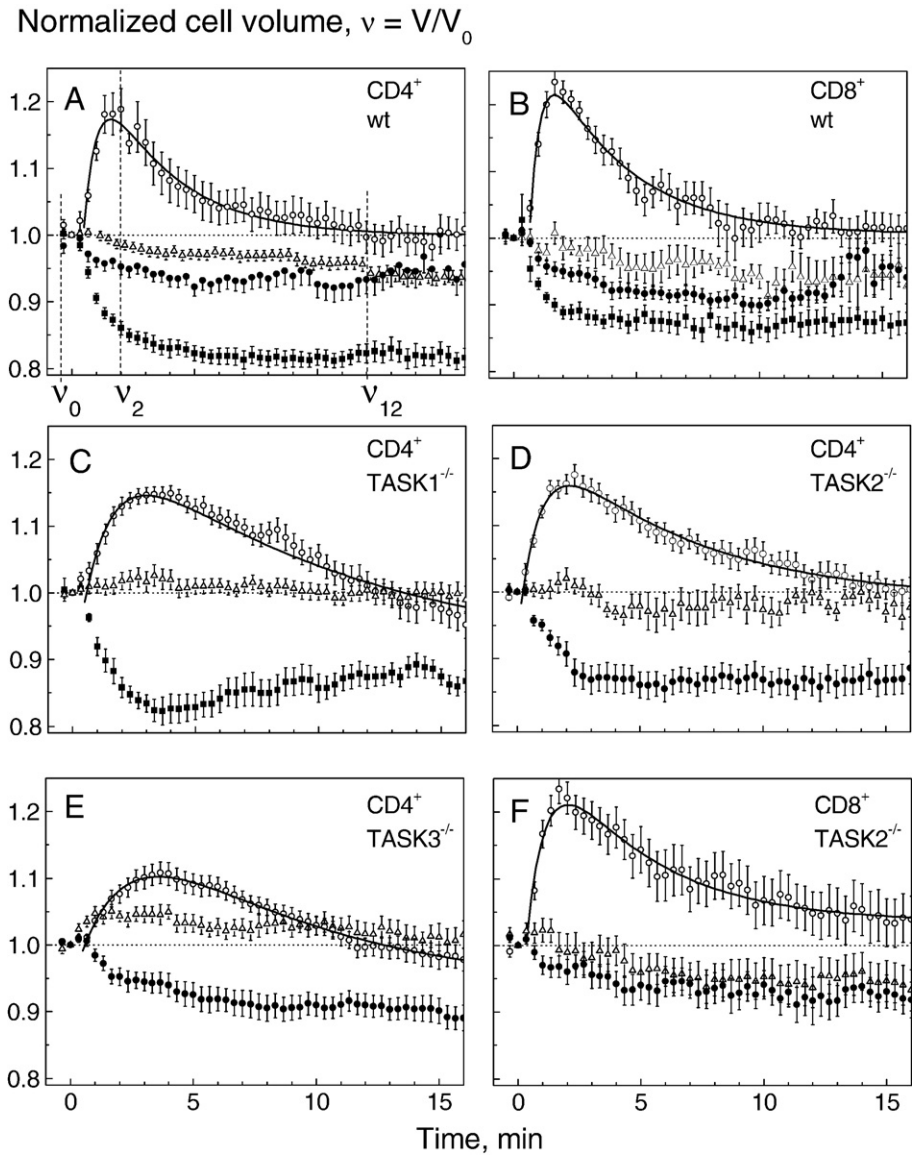

Fig. 2. Temporal changes of the normalized cell volume v in murine lymphocytes in response to PBS of varying osmolalities. The volumetric responses of $CD4^+$ and $CD8^+$ lymphocytes isolated from wild type mice are shown in A and B, respectively. The data for $CD4^+$ lymphocytes isolated from $TASK1^{-/-}$, $TASK2^{-/-}$ and $TASK3^{-/-}$ mice are given in C, D, and E, respectively. Part F includes the data of $CD8^+$ $TASK2^{-/-}$ cells. All cell samples were bathed initially in isotonic CGM (~330 mOsm) and then exposed (at $t \approx 30$ s) to PBS having osmolalities of 200, 330, 400 or 450 mOsm, indicated by *open circles*, *triangles*, *filled circles and squares*, respectively. Under hypotonic conditions (200 mOsm PBS, *open circles*), all cell phenotypes first swelled rapidly within 2–3 min and then slowly underwent partial (F) or complete RVD (A–E). Isotonic PBS caused only little – if any – volume changes. In response to hypertonic solutions with the tonicity of 400 or 450 mOsm the cells shrank rapidly during the first 2-3 min. After that, the cell volume either remained unchanged (A, B and D), slowly decreased (E and F) or increased (C, partial RVI). The initial isotonic volume is given by $v_0 = 1$. Symbols v_2 and v_{12} stand, respectively, for the normalized cell volume observed 2 and 12 min after medium exchange. Each data point represents the mean $v \pm$SE of up to ~50 individual cells (see Table 1) measured in 2–4 independent experiments. Continuous curves are best fits of the Lúcio-model to the hypotonic data (see text).

Table 1 includes, along with the experimental values v_2 and v_{12}, the osmotic properties of the plasma membrane (P_w and α) calculated with the Lúcio-model (*continuous curves* in Fig. 2). Comparison of the fitted P_w and α values does not reveal any significant differences between the two T cell subtypes derived from wild type animals with respect to their osmotic water permeability ($P_w = 1.59 \pm 0.13$ vs. 1.57 ± 0.15 μm/s in $CD4^+$ and $CD8^+$ cells, respectively) and the RVD-related solute permeability ($\alpha = 0.82 \pm 0.05$ vs. 0.86 ± 0.09 nmol s^{-1} cm^{-2}).

The osmotically inactive volume ($b \approx 0.7$) and the water permeability ($P_w \approx 1.6$ μm/s) found here for freshly isolated naive mouse T lymphocytes differ markedly from the corresponding data of cloned murine T lymphocytes L2 ($b \approx 0.28$, $P_w = 3.2$ μm/s) reported previously [9]. The discrepancy in P_w estimates can be attributed to the different theoretical models used for the evaluation of this parameter. On the other hand, the small b-value in L2 cells may result from the different osmolality range (~280–500 mOsm) and/or from the prolonged incubation of cells in hypertonic media [9], in contrast to the short-term exposure of cells (~2 min) to 200–450 mOsm PBS used here for the determination of v_2 data (Fig. 3).

In contrast to TASK1/2/3 knockout mice, which were on a C57BL/6 background, $TRESK^{-/-}$ cells were derived from C3H/HeJ mice. Therefore, the volumetric responses of $CD4^+$ cells from wild type C57BL/6 and C3H/HeJ mice were compared. The data for $CD4^+$ T lymphocytes from C3H mice are given in Supplementary Fig. S1. In contrast to the isotonic volume decrease observed in wt BL/6 cells (*triangles* in Fig. 2A), $CD4^+$ cells derived from C3H mice swelled

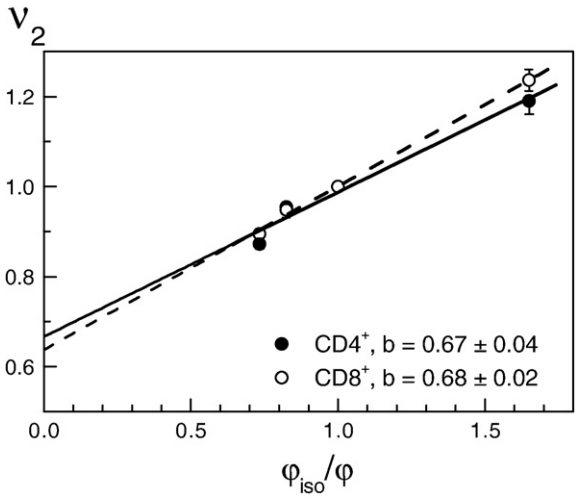

Fig. 3. Boyle van't Hoff plots for $CD4^+$ and $CD8^+$ lymphocytes (*filled* and *open circles*, respectively) derived from wild type mice. Each data point represents the mean ν_2 value ($\pm$SE, as defined in Fig. 2) plotted against the reciprocal normalized osmolality (φ_{iso}/φ, where $\varphi_{iso} = 330$ mOsm). The lines are best least-square fits of Eq. (3) to the corresponding data. The osmotically inactive volume fractions (b), defined by the y-axis-intercepts, were found to be similar in $CD4^+$ (0.67 ± 0.04) and $CD8^+$ subpopulations (0.68 ± 0.02).

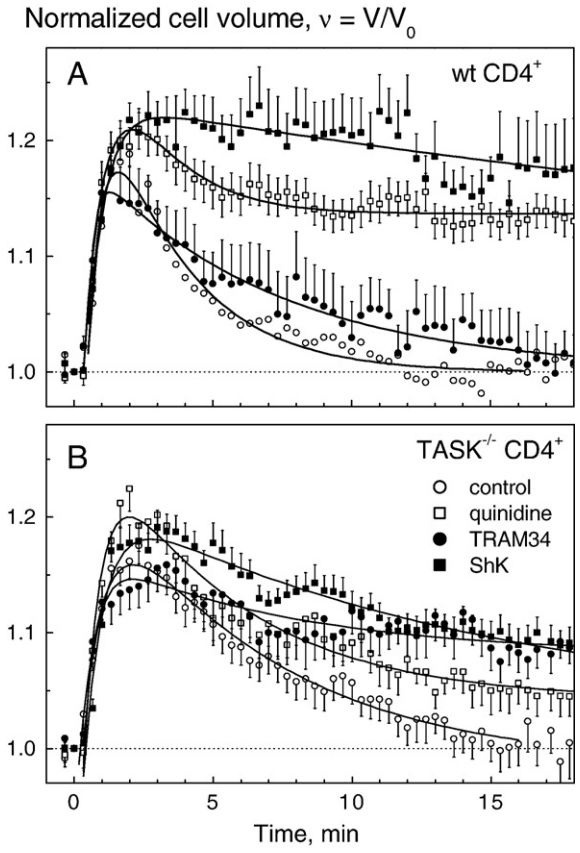

Fig. 4. Effects of potassium channel blockers on RVD of $CD4^+$ lymphocytes derived from wild type (A, wt) and $TASK2^{-/-}$ knockout mice (B, ko). The various symbols represent untreated controls (*empty circles*) and the cell samples treated with 20 μM quinidine (*empty squares*), 100 nM TRAM (*filled circles*) and 10 nM ShK (*filled squares*). All cell samples and controls were subjected to the same hypotonic stress in 200 mOsm PBS. Continuous curves are best fits of the Lúcio-model. Note that TASK2 knockout not only decreased the rate of RVD in control cells (compare *empty circles* in A and B), but also affected the relative sensitivity of RVD to potassium channel blockers. (details in Table 2).

continuously in isotonic PBS (Supplementary Fig. S1A) which was most likely due to the "leak" permeability and the uptake of NaCl. Moreover, this different genetic background reduced almost by half the rate of RVD in $CD4^+$ lymphocytes under hypotonic conditions (Fig. S1A, *open circles*), as suggested by the RVD inhibition index of $52 \pm 7\%$ given in Supplementary Table S1. The impaired RVD in C3H cells is consistent with the noticeable membrane permeability to NaCl under isotonic conditions. The response of C3H cells to hypertonic 400 mOsm PBS (i.e. osmotic shrinkage without RVI) was similar to the corresponding data of BL/6 cells discussed above (Fig. 2A, *filled circles*).

3.2. Impact of K_{2P} channel knockout on the osmoregulation of T lymphocytes

Depending on the affected protein, genetic knockout or inactivation of a K_{2P} channel exerted differential effects on the osmoregulation of murine T lymphocytes within the tonicity range of 200–450 mOsm studied here (Fig. 2C–F). Unlike wt $CD4^+$ lymphocytes, which exhibited continuous shrinkage in isotonic 330 mOsm PBS (*triangles* in Fig. 2A and B), none of the K_{2P}-deficient $CD4^+$ cell samples (including $TASK1^{-/-}$, $TASK2^{-/-}$ and $TASK3^{-/-}$) shrank in isotonic PBS (Fig. 2C–E). The lack of isotonic volume decrease implies that TASK channel knockout substantially reduced potassium leakage from the cytosol of T cells under isotonic conditions.

Comparison with the wild type control (Fig. 2A) also reveals that $TASK1^{-/-}$ lymphocytes exhibited a lower initial swelling magnitude ($\nu_2 \approx 1.15$) and a slower rate of RVD in hypotonic PBS, as clearly seen in Fig. 2C (*empty circles*). Despite obvious effects of TASK knockouts on the cell volume kinetics in hypotonic PBS (Fig. 2C–E vs. Fig. 2A), there were no statistically significant differences in the RVD inhibition index (IC_{RVD}) between wt and K_{2P}-deficient $CD4^+$ cell samples (Table 1, 5th column). For that reason we further analyzed the hypotonic data with the Lúcio-model introduced above in Section 2.4 (Eq. (2)). In terms of this model, the $TASK1^{-/-}$ related changes in the volume response are reflected by decreased values of water and solute permeability ($P_w = 0.46$ μm s^{-1}, $\alpha = 0.41$ nmol s^{-1} cm^{-2}), as compared to wt controls ($P_w = 1.59$ μm s^{-1}, $\alpha = 0.82$ nmol s^{-1} cm^{-2}; 1st line in Table 1).

Deletion of TASK2 slightly decreased the rate of RVD in $CD4^+$ lymphocytes under hypotonic conditions, without affecting significantly the volumetric behavior of these cells in hypertonic PBS (Fig. 2D). The moderate inhibition of RVD in $TASK2^{-/-}$ $CD4^+$ cells (Fig. 2D vs. A, *open circles*) is also reflected by a somewhat larger ν_{12} and a lower α value with respect to wt control (Table 1, 1st vs. 3rd line). As with $CD4^+$ lymphocytes, $TASK2^{-/-}$ $CD8^+$ cells also exhibited a delayed RVD, as compared to wt $CD8^+$ phenotype (Table 1, *bottom lines*). In iso- and hypertonic solutions, the $TASK2^{-/-}$ related changes in the volumetric behavior of $CD8^+$ cells (Fig. 2F) were qualitatively similar to those observed in $CD4^+$ lymphocytes.

Among the $CD4^+$ lymphocyte samples studied here, $TASK3^{-/-}$ cells exhibited the lowest initial swelling ($\nu_2 = 1.11$) in hypotonic PBS, which apparently was the reason for the very poor RVD-related solute permeability α (≈ 0.24 nmol s^{-1} cm^{-2}, Table 1). Unlike wt $CD4^+$ cells, $TASK3^{-/-}$ lymphocytes swelled slightly in isotonic PBS (Fig. 2E, *triangles*). In contrast, the response of $TASK3^{-/-}$ cells to hypertonic 400 mOsm saline (*filled circles*) was comparable to that of wt controls.

To examine the effects of TRESK knockout on the volume regulation in $CD4^+$ lymphocytes, these mice were compared with their corresponding wild type controls (see data of cells from C3H mice as supplementary materials in Fig. S1 and Table S1). Compared to wild type cells (Fig. S1A), TRESK knockout did not affect the hypertonic response, but slightly increased the isotonic cell swelling

(Fig. S1B). Both findings are generally consistent with the corresponding data for $K_{2P}^{-/-}$ cells from BL/6 mice shown in Fig. 2. Although TRESK$^{-/-}$ and C3H control lymphocytes exhibited quite similar percentages of RVD inhibition (46±9% vs. 52±7%), TRESK knockout reduced the RVD-related solute permeability α by about 21% (from the control value of 0.61 nmol s^{-1} cm^{-2} to 0.48 nmol s^{-1} cm^{-2}, Table S1). Despite the different genetic background (C3H vs. BL/6), the TRESK$^{-/-}$ associated decrease of α is also in agreement with the data for TASK1/2/3 knockouts summarized in Table 1.

The hypotonic data in Fig. 2 and Table 1 illustrate a significant impact of K_{2P} channel knockouts on the osmotic properties of murine T lymphocytes, including both water and solute transports. A reduced water permeability P_w appears to be a common characteristic of the plasma membrane of lymphocytes derived from K_{2P}-deficient mice. Irrespective of the affected gene, the P_w values decreased markedly (2.5–3.5 times) from 1.59 μm/s (in wt CD4$^+$) to a relatively narrow range of 0.46–0.66 μm/s in K_{2P}-deficient cells (Table 1, column 6). Despite comparable P_w values, the K_{2P}-channel deficient phenotypes differed noticeably in their RVD-related solute permeability α. Among the CD4$^+$ cell samples studied here, α values can be arranged in the following descending order (Tables 1 and S1, column 7): wild type (100%)>TRESK (~79%)>TASK2$^{-/-}$ (~73%)>TASK1$^{-/-}$ (50%)> TASK3$^{-/-}$ (~29%). The numbers in parentheses are the respective α values in percent of the corresponding BL/6 or C3H wild type control (100%). Compared to the RVD inhibition index also presented in Table 1 (column 5), the solute permeability α, calculated with the Lúcio-model, is apparently a much more useful quantity for assessing the impact of gene knockouts on the RVD-related solute transport.

3.3. Influence of potassium channel blockers on RVD in murine lymphocytes

To gain a deeper insight into the role of K_{2P} channels in the osmoregulation of T lymphocytes, we extended this study to explore a series of pharmacological agents known for their capacity to block potassium channels. Furthermore, this enabled us to address the contribution of other potassium channels which have already been suggested to play a role in volume regulation (K_V1.3 and IK_{Ca}1). The relevant data on the channel blocker concentration (and targeted protein) are available from previous electrophysiological studies [23,33–35]: quinidine 20 μM (TASK2 and to a lesser extent TRESK), ShK 10 nM (K_V1.3), and TRAM34 100 nM (IK_{Ca}1). It should be noted that quinidine may also affect K_V1.3 channels, which are known to be sensitive to its stereoisomer quinine [25,36]. Given that neither wt nor transgenic $K_{2P}^{-/-}$ lymphocytes were capable of volume regulation in hypertonic PBS media (*filled symbols* in Fig. 2), the following experiments were restricted to hypotonic conditions.

As seen in Fig. 4A, nearly all potassium channel blockers exerted significant inhibitory effects on the RVD in wt CD4$^+$ lymphocytes. Unlike K_{2P} gene knockouts (Fig. 2), channel blockers did not affect markedly the initial cell swelling. Therefore, the volumetric data in Fig. 4A allows an easy comparison of channel blockers for their RVD inhibition capacities (IC_{RVD}). Substitution of the experimental ν_{12} and ν_2 data (Table 2) into Eq. (1) gives the following order of IC_{RVD} values: ShK>quinidine>TRAM. This sequence suggests a major contribution of K_V1.3 and TASK2/TRESK channels to the RVD in the wild type CD4$^+$ cells, whereas IK_{Ca}1 appears to play a secondary role in the hypotonic volume regulation of the wt cells.

In addition to its effects on RVD discussed above (Fig. 2D), TASK2 knockout markedly altered the sensitivity of RVD to potassium channel blockers (Fig. 4B). Thus, in contrast to the nearly complete inhibition of RVD in wt CD4$^+$ cells treated with the K_V1.3 channel blocker ShK ($IC_{RVD}\approx 80\%$), the same ShK concentration impaired RVD in TASK2$^{-/-}$ cells to a lesser extent ($IC_{RVD}\approx 60\%$, *filled squares* in Fig. 4B). As expected, TASK2 knockout significantly attenuated the RVD inhibitory activity of the TASK2 channel blocker quinidine (*empty squares* in Fig. 4), which is suggested by a decreased IC_{RVD} value of ~30% (vs. 75% in wt cells). TASK2 knockout, however, had quite the opposite effect on the RVD sensitivity to TRAM. In this case, IC_{RVD} increased almost tenfold from 6% in wt to ~60% in TASK2$^{-/-}$ cells (Table 2).

Taken together, the combination of genetic and pharmacological approaches provided clear evidence for the involvement of various potassium channels (most notably K_V1.3 and TASK2) in the RVD of mouse T lymphocytes exposed to hypotonic saline. Genetic knockout of TASK2 not only exerted a moderate inhibitory effect on the RVD in mouse lymphocytes but also modified the expression pattern of other potassium channels involved in the osmotic volume regulation. The latter effect caused large alterations in the pharmacological profile of RVD inhibition.

3.4. Significance of K_{2P} channels for the cell volume regulation

The expression of members of K_{2P} channel family in murine and human T lymphocytes has only been described a few years ago [23–25]. In the present study we succeeded in integrating these channels into the existing models of T cell volume regulation (Fig. 5), which until now relied on only two other potassium channels (K_V1.3 and IK_{Ca}1). In agreement with our data for TASK2 reported here, an important role of TASK2 in volume regulation processes has been described before in other cell types. Thus, volume regulation in kidney cells depends strongly on TASK2 [37,38] and genetic deletion of TASK2 abolishes the downstream events, caspase activation and cell death upon apoptotic volume decrease. Furthermore, TASK2 is involved in the volume regulation of spermatozoa (which are physiologically confronted with a broad range of extracellular osmolalities [39]), and also in the osmoregulation of Ehrlich ascites tumor cells [40,41].

Even more data on the involvement of TRESK in cell volume regulation are available in the current literature. The expression of TRESK channels in a human lymphoma cell line (Jurkat cells) and their importance (together with K_V1.3) for the apoptotic volume decrease have been recently shown elsewhere [25,26]. However, potassium channels expressed in Jurkat cells are quite different from those in

Table 1
Impact of K_{2P} knockout on the osmotic properties of murine CD4$^+$ and CD8$^+$ lymphocytes in PBS of reduced osmolality (200 mOsm).

CD phenotype	Mutation	$\nu_2 \pm$ SE	$\nu_{12} \pm$ SE	$IC_{RVD} \pm$ SE[a] %	$P_w \pm$ SE μm/s	α ± SE nmol/s cm^2	N cell number
CD4$^+$	wt	1.19 ± 0.03	1.00 ± 0.02	0 ± 8	1.59 ± 0.13	0.82 ± 0.05	38
CD4$^+$	TASK1$^{-/-}$	1.15 ± 0.01	1.00 ± 0.01	0 ± 7	0.46 ± 0.08	0.41 ± 0.04	13
CD4$^+$	TASK2$^{-/-}$	1.16 ± 0.02	1.02 ± 0.01	13 ± 6	0.59 ± 0.07	0.60 ± 0.04	38
CD4$^+$	TASK3$^{-/-}$	1.11 ± 0.01	1.00 ± 0.01	0 ± 9	0.66 ± 0.03	0.24 ± 0.01	28
CD8$^+$	wt	1.24 ± 0.02	1.01 ± 0.02	4 ± 4	1.57 ± 0.15	0.86 ± 0.09	48
CD8$^+$	TASK2$^{-/-}$	1.24 ± 0.03	1.05 ± 0.02	21 ± 9	1.09 ± 0.15	0.61 ± 0.04	27

[a] RVD inhibition index *IC*RVD was calculated with Eq. (1) using the corresponding data for $\nu = 1$, ν_2 and ν_{12} defined in Fig. 2.

Table 2
Effects of potassium channel blockers on the volumetric response of murine CD4$^+$ lymphocytes in 200 mOsm PBS.

Cell phenotype	Channel blocker, concentration	Targeted channel	$\nu_2 \pm$ SE	$\nu_{12} \pm$ SE	$IC_{RVD} \pm$ SE %	N cell number
wt	Untreated control		1.19 ± 0.03	1.00 ± 0.02	0 ± 8	38
wt	20 μM quinidine	TASK2	1.20 ± 0.03	1.15 ± 0.02	75 ± 9	40
wt	100 nM TRAM34	$IK_{Ca}1$	1.16 ± 0.03	1.01 ± 0.04	6 ± 10	17
wt	10 nM ShK	$K_V1.3$	1.22 ± 0.02	1.17 ± 0.04	77 ± 11	22
TASK2$^{-/-}$	Untreated control		1.16 ± 0.02	1.02 ± 0.01	13 ± 6	38
TASK2$^{-/-}$	20 μM quinidine	TASK2	1.22 ± 0.02	1.07 ± 0.02	32 ± 10	20
TASK2$^{-/-}$	100 nM TRAM34	$IK_{Ca}1$	1.16 ± 0.02	1.10 ± 0.02	63 ± 15	27
TASK2$^{-/-}$	10 nM ShK	$K_V1.3$	1.18 ± 0.01	1.11 ± 0.01	61 ± 7	31

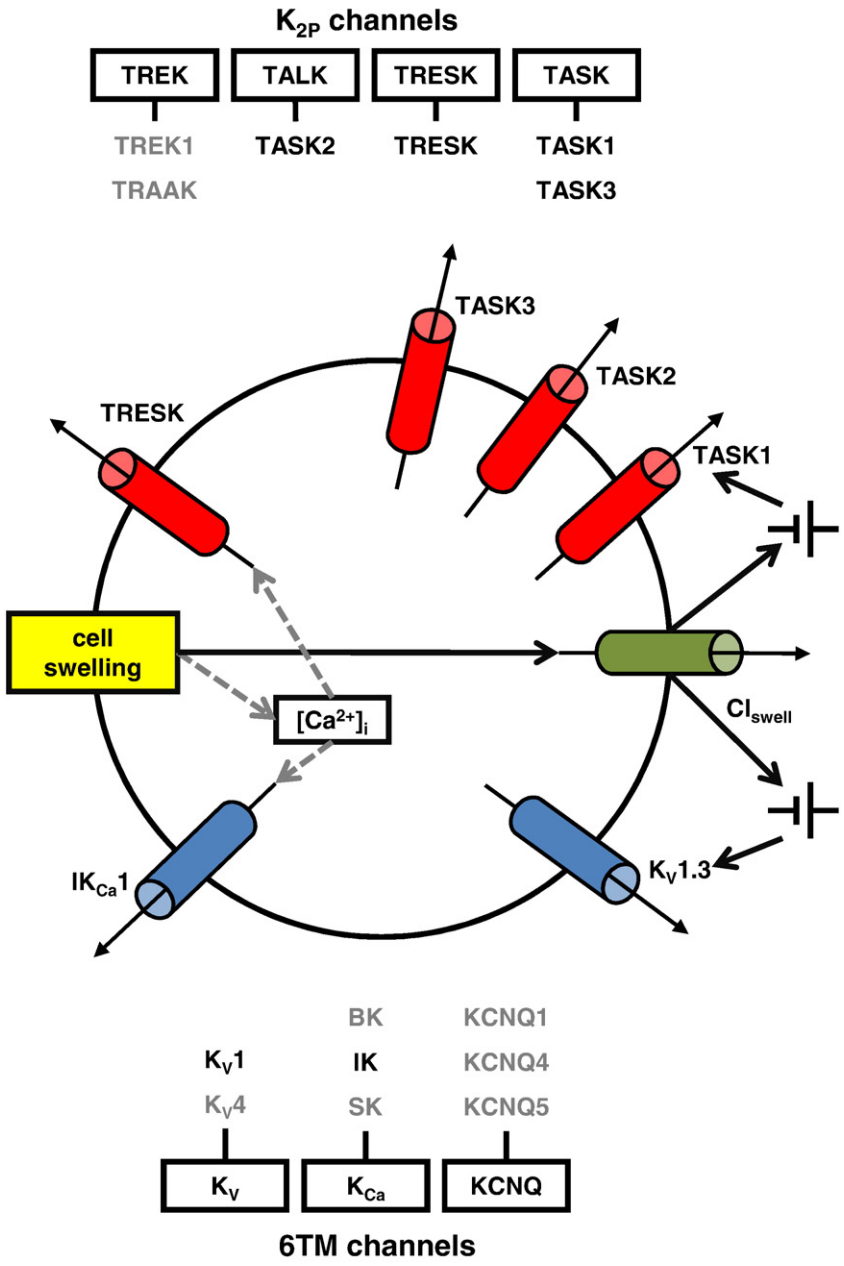

Fig. 5. Scheme of RVD in T lymphocytes. The events following a hypotonic shock with subsequent cell swelling are shown: the opening of swelling-activated chloride channels (Cl_{swell}) depolarizes the membrane potential towards the chloride-equilibrium potential of −35 mV which activates voltage-gated potassium channels ($K_V1.3$) and enhances the driving force for the K_{2P} channels TASK1, TASK2 and TASK3. An additional involvement of the Ca^{2+}-activated channels $IK_{Ca}1$ and TRESK has been suggested previously. Our results indicate a predominant role of different channels under diverse conditions. All potassium channels from the family of K_{2P} channels (upper side) and 6 transmembrane domain (6TM) channel family (lower side) which have been shown to be able to mediate volume regulation are listed (modified from Ref. [3]). Channels relevant for lymphocytes are highlighted in black.

primary T cells (e.g. small conductance $K_{Ca}2.2$, TRPM2 and TRPM4 [42–44]). Our finding that TRESK$^{-/-}$ cells display an impaired RVD (Supplementary Fig. S1B) support the concept of a functional role of TRESK channels in the osmoregulation of mouse T cells.

In summary, our data provide evidence that two-pore domain potassium channels are involved in RVD of T lymphocytes, which is particularly reflected by a reduced solute permeability α in $K_{2P}^{-/-}$ cells (Table 1). The expression profile of ion channels in T lymphocytes, however, varies widely between different T cell subtypes and the activation status of individual cells. It is therefore plausible to assume that the varying results in our study reflect the expression status and ion channel repertoire of different cell types. Among the various potassium channels, $K_V1.3$ and TASK2 appear to be mainly responsible for RVD in murine T lymphocytes. Fig. 5 schematically illustrates a T cell expressing the diverse potassium and chloride channel pools involved in hypotonic volume regulation.

3.5. Concluding remarks

As a basic and mandatory physiological mechanism, volume regulation relies apparently on a complex and redundant network of potassium channels, including most notably 6TM and K_{2P} families, whose expression and open probability are governed by a great number of factors discussed above. Further studies are necessary to elucidate in detail the role of K_{2P} channels in volume regulation.

The response of T and other immune cells to anisotonic solutions is not only of physiological but also of biotechnological interest. This is because hypotonic sugar solutions are useful in the production of therapeutically relevant hybrid cells via electrofusion, and also for electrotransfection of mammalian cells [45,46]. Finally, strongly anisotonic media are also widely used in cryo- and lyopreservation of rare and valuable mammalian cells and tissues [47,48].

Supplementary materials related to this article can be found online at doi:10.1016/j.bbamem.2011.04.013.

Acknowledgements

The authors declare no conflict of interest. We are grateful to Douglas A. Bayliss (Department of Pharmacology, University of Virginia, Charlottesville, Virginia, USA) for providing TASK1$^{-/-}$ and TASK3$^{-/-}$ mice and to Jacques Barhanin (Institut de Pharmacologie Moléculaire et Cellulaire, Antipolis, France) for providing TASK2$^{-/-}$ mice. We thank Marcus Behringer (Biotechnology & Biophysics, Wuerzburg) for manufacturing the PDMS chambers used in volumetric experiments. This work was supported by Interdisziplinaeres Zentrum für klinische Forschung (Interdisciplinary Center for Clinical Research A-54-1, S.G.M., H.W.; Bud3/010/10, T.B.), the Deutsche Forschungsgemeinschaft (SFB 581, TP A10, S.G.M.; FOR1086, TP2, T.B., S.G.M.) and by the BMBF (16SV2387, V.L.S.).

References

[1] F. Lang, G.L. Busch, M. Ritter, H. Völkl, S. Waldegger, E. Gulbins, D. Häussinger, Functional significance of cell volume regulatory mechanisms, Physiol. Rev. 78 (1998) 247–306.
[2] F. Lang, G.L. Busch, H. Völkl, The diversity of volume regulatory mechanisms, Cell. Physiol. Biochem. 8 (1998) 1–45.
[3] E.K. Hoffmann, I.H. Lambert, S.F. Pedersen, Physiology of cell volume regulation in vertebrates, Physiol. Rev. 89 (2009) 193–277.
[4] M.D. Cahalan, K.G. Chandy, The functional network of ion channels in T lymphocytes, Immunol. Rev. 231 (2009) 59–87.
[5] S. Grinstein, C.A. Clarke, A. Dupre, A. Rothstein, Volume-induced increase of anion permeability in human lymphocytes, J. Gen. Physiol. 80 (1982) 801–823.
[6] R.S. Lewis, P.E. Ross, M.D. Cahalan, Chloride channels activated by osmotic stress in T lymphocytes, J. Gen. Physiol. 101 (1993) 801–826.
[7] M.D. Cahalan, H. Wulff, K.G. Chandy, Molecular properties and physiological roles of ion channels in the immune system, J. Clin. Immunol. 21 (2001) 235–252.
[8] C. Deutsch, L.Q. Chen, Heterologous expression of specific K+channels in T lymphocytes: functional consequences for volume regulation, Proc. Natl. Acad. Sci. U. S. A. 90 (1993) 10036–10040.
[9] S.C. Lee, M. Price, M.B. Prystowsky, C. Deutsch, Volume response of quiescent and interleukin 2-stimulated T-lymphocytes to hypotonicity, Am. J. Physiol. 254 (1988) C286–C296.
[10] S. Grinstein, J.D. Smith, Calcium-independent cell volume regulation in human lymphocytes. Inhibition by charybdotoxin, J. Gen. Physiol. 95 (1990) 97–120.
[11] S. Grinstein, J.D. Smith, Ca^{2+} induces charybdotoxin-sensitive membrane potential changes in rat lymphocytes, Am. J. Physiol. 257 (1989) C197–C206.
[12] R. Khanna, M.C. Chang, W.J. Joiner, L.K. Kaczmarek, L.C. Schlichter, hSK4/hIK1, a calmodulin-binding KCa channel in human T lymphocytes. Roles in proliferation and volume regulation, J. Biol. Chem. 274 (1999) 14838–14849.
[13] L.C. Schlichter, G. Sakellaropoulos, Intracellular Ca^{2+} signalling induced by osmotic shock in human T lymphocytes, Exp. Cell Res. 215 (1994) 211–222.
[14] P.E. Ross, M.D. Cahalan, Ca^{2+} influx pathways mediated by swelling or stores depletion in mouse thymocytes, J. Gen. Physiol. 106 (1995) 415–444.
[15] S. Grissmer, S. Ghanshani, B. Dethlefs, J.D. McPherson, J.J. Wasmuth, G.A. Gutman, M.D. Cahalan, K.G. Chandy, The Shaw-related potassium channel gene, $K_v3.1$, on human chromosome 11, encodes the type l K^+ channel in T cells, J. Biol. Chem. 267 (1992) 20971–20979.
[16] R.S. Lewis, M.D. Cahalan, Subset-specific expression of potassium channels in developing murine T lymphocytes, Science 239 (1988) 771–775.
[17] M.D. Cahalan, K.G. Chandy, Ion channels in the immune system as targets for immunosuppression, Curr. Opin. Biotechnol. 8 (1997) 749–756.
[18] M. Prakriya, R.S. Lewis, Separation and characterization of currents through store-operated CRAC channels and Mg^{2+}-inhibited cation (MIC) channels, J. Gen. Physiol. 119 (2002) 487–507.
[19] T. Numata, T. Shinizu, Y. Okada, TRPM7 is a stretch- and swelling-activated cation channel involved in volume regulation in human epithelial cells, Am. J. Physiol. Cell Physiol. 292 (2007) C460–C467.
[20] J.J. García, R. Sánchez Olea, H. Pasantes-Morales, Taurine release associated to volume regulation in rabbit lymphocytes, J. Cell. Biochem. 45 (1991) 207–212.
[21] V.L. Sukhorukov, D. Imes, M.W. Woellhaf, J. Andronic, M. Kiesel, R. Shirakashi, U. Zimmermann, H. Zimmermann, Pore size of swelling-activated channels for organic osmolytes in Jurkat lymphocytes, probed by differential polymer exclusion, Biochim. Biophys. Acta 1788 (2009) 1841–1850.
[22] M. Kiesel, R. Reuss, J. Endter, D. Zimmermann, H. Zimmermann, R. Shirakashi, E. Bamberg, U. Zimmermann, V.L. Sukhorukov, Swelling-activated pathways in human T-lymphocytes studies by cell volumetry and electrorotation, Biophys. J. 90 (2006) 4720–4729.
[23] S. Bittner, N. Bobak, A.M. Herrmann, K. Göbel, P. Meuth, K.G. Höhn, M.P. Stenner, T. Budde, H. Wiendl, S.G. Meuth, Upregulation of $K_{2P}5.1$ potassium channels in multiple sclerosis, Ann. Neurol. 68 (2010) 58–69.
[24] S.G. Meuth, S. Bittner, P. Meuth, O.J. Simon, T. Budde, H. Wiendl, TWIK-related acid-sensitive K+channel 1 (TASK1) and TASK3 critically influence T lymphocyte effector functions, J. Biol. Chem. 283 (2008) 14559–14570.
[25] I.I. Pottosin, E. Bonales-Alatorre, G. Valencia-Cruz, M.L. Mendoza-Magaña, O.R. Dobrovinskaya, TRESK-like potassium channels in leukemic T cells, Pflugers Arch. 456 (2008) 1037–1048.
[26] G. Valencia-Cruz, L. Shabala, I. Delgado-Enciso, S. Shabala, E. Bonales-Alatorre, I.I. Pottosin, O.R. Dobrovinskaya, K(bg) and $K_v1.3$ channels mediate potassium efflux in the early phase of apoptosis in Jurkat T lymphocytes, Am. J. Physiol. Cell Physiol. 297 (2009) C1544–C1553.
[27] H. Zheng, J.H. Nam, B. Pang, D.H. Shin, J.S. Kim, Y.S. Chun, J.W. Park, H. Bang, W.K. Kim, Y.E. Earm, S.J. Kim, Identification of the large-conductance background K^+ channel in mouse B cells as TREK-2, Am. J. Physiol. Cell Physiol. 297 (2009) C188–C197.
[28] T. Dobler, A. Springauf, S. Tovornik, M. Weber, A. Schmitt, R. Sedlmeier, E. Wischmeyer, F. Döring, TRESK two-pore-domain K^+ channels constitute a significant component of background potassium currents in murine dorsal root ganglion neurones, J. Physiol. 15 (2007) 867–879.
[29] D.K. Mulkey, E.M. Talley, R.L. Stornetta, A.R. Siegel, G.H. West, X. Chen, N. Sen, A.M. Mistry, P.G. Guyenet, D.A. Bayliss, TASK channels determine pH sensitivity in select respiratory neurons but do not contribute to central respiratory chemosensitivity, J. Neurosci. 19 (2007) 4049–4058.
[30] H. Barriere, R. Belfodil, I. Rubera, M. Tauc, F. Lesage, C. Poujeol, N. Guy, J. Barhanin, P. Poujeol, Role of TASK2 potassium channels regarding volume regulation in primary cultures of mouse proximal tubules, J. Gen. Physiol. 122 (2003) 177–190.
[31] A.D. Lúcio, R.A. Santos, O.N. Mesquita, Measurements and modeling of water transport and osmoregulation in a single kidney cell using optical tweezers and videomicroscopy, Phys. Rev. E Stat. Nonlin. Soft Matter Phys. 68 (2003) 041906.
[32] S. Grinstein, A. Rothstein, B. Sarkadi, E.W. Gelfand, Responses of lymphocytes to anisotonic media: volume-regulating behavior, Am. J. Physiol. 246 (1984) C204–C215.
[33] H. Wulff, M.J. Miller, W. Hansel, S. Grissmer, M.D. Cahalan, K.G. Chandy, Design of a potent and selective inhibitor of the intermediate-conductance Ca^{2+}-activated K^+ channel, $IK_{Ca}1$: a potential immunosuppressant, Proc. Natl. Acad. Sci. U. S. A. 97 (2000) 8151–8156.
[34] S.G. Meuth, M.I. Aller, T. Munsch, T. Schuhmacher, T. Seidenbecher, P. Meuth, C. Kleinschnitz, H.C. Pape, H. Wiendl, W. Wisden, T. Budde, The contribution of TWIK-related acid-sensitive K+-containing channels to the function of dorsal lateral geniculate thalamocortical relay neurons, Mol. Pharmacol. 69 (2006) 1468–1476.
[35] K.G. Chandy, H. Wulff, C. Beeton, M. Pennington, G.A. Gutman, M.D. Cahalan, K^+ channels as targets for specific immunomodulation, Trends Pharmacol. Sci. 25 (2004) 280–289.

[36] G.A. Gutman, K.G. Chandy, S. Grissmer, M. Lazdunski, D. McKinnon, L.A. Pardo, G.A. Robertson, B. Rudy, M.C. Sanguinetti, W. Stühmer, X. Wang, International Union of Pharmacology. LIII. Nomenclature and molecular relationships of voltage-gated potassium channels, Pharmacol. Rev. 57 (2005) 473–508.
[37] H. Barriere, R. Belfodil, I. Rubera, M. Tauc, F. Lesage, C. Poujeol, N. Guy, J. Barhanin, P. Poujeol, Role of TASK2 potassium channels regarding volume regulation in primary cultures of mouse proximal tubules, J. Gen. Physiol. 122 (2003) 177–190.
[38] S. L'Hoste, M. Poet, C. Duranton, R. Belfodil, H. é Barriere, I. Rubera, M. Tauc, C. Poujeol, J. Barhanin, P. Poujeol, Role of TASK2 in the control of apoptotic volume decrease in proximal kidney cells, J. Biol. Chem. 282 (2007) 36692–36703.
[39] T.G. Cooper, C.H. Yeung, Involvement of potassium and chloride channels and other transporters in volume regulation by spermatozoa, Curr. Pharm. Des. 13 (2007) 3222–3230.
[40] M.I. Niemeyer, L.P. Cid, L.F. Barros, F.V. Sepulveda, Modulation of the two-pore domain acid-sensitive K^+ channel TASK-2 (KCNK5) by changes in cell volume, J. Biol. Chem. 276 (2001) 43166–43174.
[41] M.I. Niemeyer, L.P. Cid, F.V. Sepulveda, K^+ conductance activated during regulatory volume decrease. The channels in Ehrlich cells and their possible molecular counterpart, Comp. Biochem. Physiol. A Mol. Integr. Physiol. 130 (2001) 565–575.
[42] H. Jäger, J.P. Adelman, S. Grissmer, SK2 encodes the apamin-sensitive Ca^{2+}-activated K^+ channels in the human leukemic T cell line, Jurkat, FEBS Lett. 469 (2000) 192–202.
[43] P. Launay, H. Cheng, S. Srivatsan, R. Penner, A. Fleig, J.P. Kinet, TRPM4 regulates calcium oscillations after T cell activation, Science 306 (2004) 1374–1377.
[44] A. Beck, M. Kolisek, L.A. Bagley, A. Fleig, R. Penner, Nicotinic acid adenine dinucleotide phosphate and cyclic ADP-ribose regulate TRPM2 channels in T lymphocytes, FASEB J. 20 (2006) 962–964.
[45] V.L. Sukhorukov, R. Reuss, D. Zimmermann, C. Held, K.J. Müller, M. Kiesel, P. Gessner, A. Steinbach, W.A. Schenk, E. Bamberg, U. Zimmermann, Surviving high-intensity field pulses: strategies for improving robustness and performance of electrotransfection and electrofusion, J. Membr. Biol. 206 (2005) 187–201.
[46] V.L. Sukhorukov, R. Reuss, J. Endter, S. Fehrmann, A. Katsen-Globa, P. Geβner, A. Steinbach, K.J. Müller, A. Karpas, U. Zimmermann, H. Zimmermann, A biophysical approach to the optimisation of dendritic-tumour cell electrofusion, Biochem. Biophys. Res. Commun. 346 (2006) 829–839.
[47] R. Shirakashi, R. Reuss, J. Ludwig, F. Ehrhart, U. Zimmermann, V.L. Sukhorukov, Introduction of lyo- and cryoprotective carbohydrates into mammalian cells through swelling-activated channels, Trans. Japan Soc. Mech. Eng. B71 (2005) 901–907.
[48] S.M. Zeisberger, J.C. Schulz, M. Mairhofer, P. Ponsaerts, G. Wouters, D. Doerr, A. Katsen-Globa, M. Ehrbar, J. Hescheler, S.P. Hoerstrup, A.H. Zisch, A. Kolbus, H. Zimmermann, Biological and physicochemical characterization of a serum- and xeno-free chemically defined cryopreservation procedure for adult human progenitor cells, Cell Transplant. (2010), doi:10.3727/096368910X547426.